International Journal of Mechanical and Electrical Engineering
ISSN: 3005-9615 (Print), ISSN: 3005-7132 (Online) | Volume 8, Number 2, Year 2026
DOI: https://doi.org/10.62051/ijmee.v8n2.06
Journal homepage: https://wepub.org/index.php/IJMEE/index

Static Modeling and Parameter Impact Analysis of the Bearing System in RV Reducers

Yingjian Tang *

Tianjin University of Technology and Education, Tianjin, China
* Corresponding Author: Yingjian Tang

ABSTRACT

The RV reducer is a critical transmission component in industrial robot joints, whose bearing system's mechanical performance directly affects the overall machine's lifespan and reliability. This study establishes a complete static model of the RV reducer, incorporating deformation compatibility conditions and force equilibrium equations. Through numerical simulation, the effects of manufacturing errors and key structural parameters on bearing forces are analyzed. The results show that radial and angular errors significantly alter the load distribution on the crankpin bearings, increasing the force amplitude, while having minimal impact on the output bearings. Increasing the eccentricity reduces the maximum bearing force, whereas variations in the pin gear center circle radius have a relatively minor influence on the force trends. This research provides a theoretical basis for the design and performance optimization of RV reducers.

KEYWORDS

RV Reducer; Bearing Statics; Deformation Compatibility; Error Analysis.

1. INTRODUCTION

Since the 1980s, when the Japanese company Teijin developed the concept of cycloidal-pin planetary transmission proposed by Laurens Broll, the RV (Rotate Vector) reducer has evolved over half a century[1]. Known for its high motion accuracy, smooth transmission, and wide range of transmission ratios, the RV reducer is widely used in industrial robot joints[2]. The bearing between the crankshaft and the cycloidal gear is a critical load-carrying component in the RV reducer responsible for transmitting torque. As the weakest link in the system, its service life directly determines the lifespan of the RV reducer[3]. Accurately obtaining the force variation acting on the bearing and calculating its deformation and stress based on these forces are prerequisites for studying its service life.

Both domestic and international scholars have conducted extensive research on RV reducers. Reference [4] proposes a force calculation method based on multi-body dynamics and investigates the influence of input speed and load on the crankpin bearing force. Reference [5] employs the intimate value method to analyze the impact of various parameters on meshing forces, enabling a ranking of their influence in a straightforward, convenient, and reliable manner. Reference [6] establishes a three-dimensional model of the RV reducer, performs dynamic analysis, derives the rotational speeds at each transmission stage, and validates the model's accuracy by comparing the results with simulations. Reference [7] calculates the forces acting on the cycloidal gear–pin teeth mechanism and the cycloidal gear support bearings, obtaining curves of the meshing force between the cycloidal gear and pin teeth as well as the support bearing force versus the crankshaft rotation angle, and verifies the data accuracy through modeling and simulation in UG.

Starting from the structure and transmission principle of the RV reducer, and based on deformation compatibility conditions, this paper analyzes the forces on key bearings within the RV reducer. It further examines the bearing forces considering positional errors in the crankshaft bearing bores, as well as changes in the forces resulting from variations in key component parameters.

2. MECHANICAL ANALYSIS

2.1. RV Reducer Structure

The RV reducer is a two-stage enclosed planetary transmission system composed of involute and cycloidal gears. Its kinematic schematic is illustrated in Figure 1. In this gear train, the involute gears form a K-H type differential gear train, consisting of a sun gear 1, three radially equally spaced planet gears, and a carrier (planet carrier). The cycloidal gears constitute a K-H-V type planetary gear train, comprising three radially equally spaced crankshafts 3, two symmetrically arranged cycloidal gears 4 and 4′, a set of needle teeth 5, and an output plate 6. The carrier 7 and the output plate 6 are integrated into a single component.

During motion transmission within this gear train, the planet gears drive the rotation of the crankshafts. The crankshafts transfer the rotation of the planet gears to the cycloidal gears, causing them to undergo revolution. Subsequently, the cycloidal gears transmit their own rotation back to the carrier (which is fixedly connected to the output plate) via the output plate. This rotation serves as the input motion for the differential gear train, thereby forming a closed-loop planetary transmission system. A structural block diagram of this system is provided in the accompanying figure.

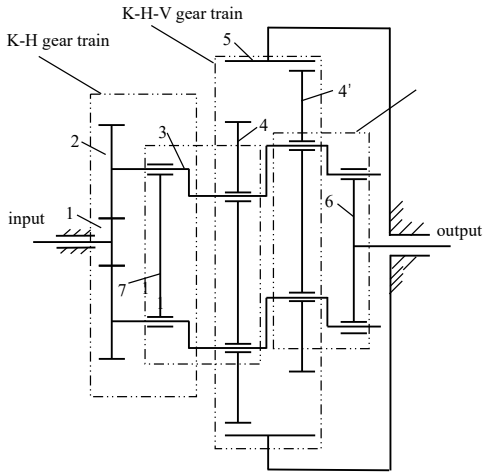

1. Sun Gear 2. Planetary Gear 3. Crankshaft 4 (4a'). Cycloidal Gear

5. Pin Gear (or Needle Gear)6. Output Plate (or Output Flange) 7. Carrier (or Planet Carrier)

Figure 1. Schematic diagram of the RV reducer mechanism

2.2. Deformation Compatibility Conditions

Due to the structural characteristics of the RV reducer, establishing appropriate deformation compatibility conditions is a prerequisite for conducting static analysis.

(1) The sun gear and planet gears. The planet gears are uniformly distributed along the circumference. When an input torque T_{in} is applied to the sun gear, it is assumed that the sun gear meshes simultaneously with all planet gears. The resulting deformation displacement along the line of action (or mesh direction) is given

$$\delta_{sp1} = \delta_{sp2} = \delta_{sp3} \tag{1}$$

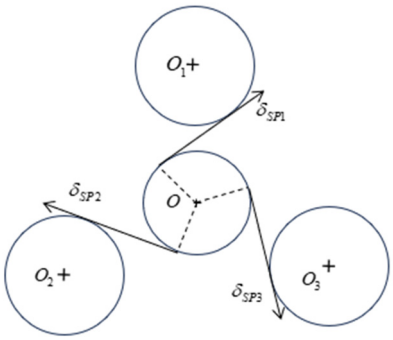

Figure 2. Force analysis of the sun gear and planet gear

(2) Cycloidal gears.Similar to the deformation compatibility analysis for the planetary gears, it can be approximately assumed that the deformation of each cycloidal gear along the line of action is equal. Thus, the deformation compatibility condition for the cycloidal gears is:

$$\delta_{cr1} = \delta_{cr2} = \delta_{cr3} \tag{2}$$

(3) Crankpin bearings.Due to the high rigidity of the cycloidal gears and crankshafts, it can be assumed that the crankpin bearings undergo elastic deformation under the influence of the mesh force from the needle teeth and the load torque. When manufacturing errors are taken into account, the deformation compatibility condition for the crankpin bearings is:

$$\begin{cases} \delta_1 + \Delta\delta_1 = \delta_2 + \Delta\delta_2 = \delta_3 + \Delta\delta_3 \\ \delta_{t1} + \Delta\delta_{t1} = \delta_{t2} + \Delta\delta_{t2} = \delta_{t3} + \Delta\delta_{t3} \end{cases} \tag{3}$$

where:

$$\begin{cases} \Delta\delta_i = E_{Ci} \sin\left(\beta_{\delta Ci} + \dfrac{2(i-1)pi}{3}\right) \\ \Delta\delta_{ti} = E_{Ci} \sin\left(\dfrac{\mathrm{pi}}{2} - \beta_{\delta Ci} + \arctan(K_y)\right) \end{cases} \tag{4}$$

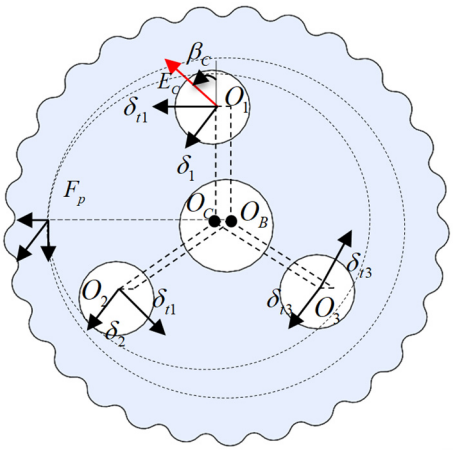

Figure 3. Elastic deformation of the swivel arm bearing

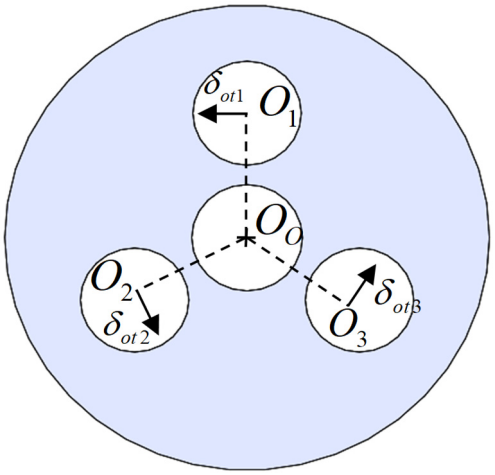

Figure 4. Elastic deformation of the support bearing

(4) Support bearings. Due to the high rigidity of the output plate, it can be assumed that the support bearings undergo elastic deformation under the influence of the external load torque. When manufacturing errors are taken into account, the deformation compatibility condition for the support bearings is:

$$\delta_{ot1} + \Delta\delta_{ot1} = \delta_{ot2} + \Delta\delta_{ot2} = \delta_{ot3} + \Delta\delta_{ot3} \tag{5}$$

where:

$$\Delta\delta_{oti} = E_{hi} \sin(\beta_{\delta Hi}) \tag{6}$$

2.3. Static Equilibrium Equations

(1) Sun gear and planet gears. The sun gear is subjected to the input torque and the forces exerted by the planet gears. The static equilibrium equations can be formulated as follows:

$$\begin{cases} \sum_{i=1}^{3} F_{psi} r_s = T_s \\ F_{ps1} = F_{ps2} = F_{ps3} \end{cases} \tag{7}$$

The sun gear is subjected to the input torque and the forces exerted by the planet gears. The static equilibrium equations can be formulated as follows:

$$\begin{cases} F_{\mathrm{spi}} r_{\mathrm{p}} = T_{\mathrm{Hpi}} \\ F_{\mathrm{spi}} = F_{\mathrm{Hpi}} \end{cases} \tag{8}$$

(2)Cycloidal gears and pin gear. The cycloidal gear is subjected to the forces F_{px} and F_{py} from the pin gear, as well as the forces exerted by each crankshaft. For analytical clarity, the crankshaft forces are decomposed into components F_{Hicj1}, F_{Hicj2} , and $FHicj3$ .Here, $\sum F_{Hicj1}$ is responsible for balancing the moments, while $\sum F_{Hicj2}$,$\sum F_{Hicj3}$ are responsible for balancing the forces. Therefore, the static equilibrium equations are as follows:

$$\begin{cases} \sum_{i=1}^{3} F_{Hicj2} = F_{px} \\ \sum_{i=1}^{3} F_{Hicj3} = F_{py} \\ \sum_{i=1}^{3} F_{Hicj1}(r_s + r_p) = F_{px} r_c \end{cases} \tag{9}$$

$$\begin{cases} F_x = \dfrac{T_b}{2K_1 r_b} \\ F_y = K_y F \\ K_y = \dfrac{2}{\pi}\left[\dfrac{1}{K_1} + \dfrac{K_1^2 - 1}{2K_1^2}\ln\left(\dfrac{1+K_1}{1-K_1}\right)\right] \end{cases} \tag{10}$$

where:

K_y is the short-width coefficient,

r_b is the pitch circle coefficient of the pin gear,

T_b is the external torque applied to the pin gear.

From the deformation compatibility conditions, the following can be derived:

$$\begin{cases} \dfrac{F_1}{k} + \Delta\delta_1 = \dfrac{F_2}{k} + \Delta\delta_2 = \dfrac{F_3}{k} + \Delta\delta_3 \\ \dfrac{F_{t1}}{k} + \Delta\delta_{t1} = \dfrac{F_{t2}}{k} + \Delta\delta_{t2} = \dfrac{F_{t3}}{k} + \Delta\delta_{t3} \end{cases} \tag{11}$$

where:

$$\begin{cases} R = F \\ k = 0.34 \times 10^4 (R^{0.1} Z^{0.9} L^{0.8} \cos^{1.9} \partial) \end{cases} \tag{12}$$

where:

k denotes the bearing stiffness,

Z represents the number of rollers;

L refers to the effective length of the rollers;

φ indicates the contact angle of the rolling elements.

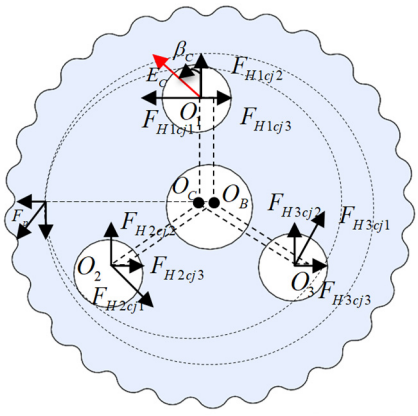

Figure 5. Force analysis of the cycloidal gear

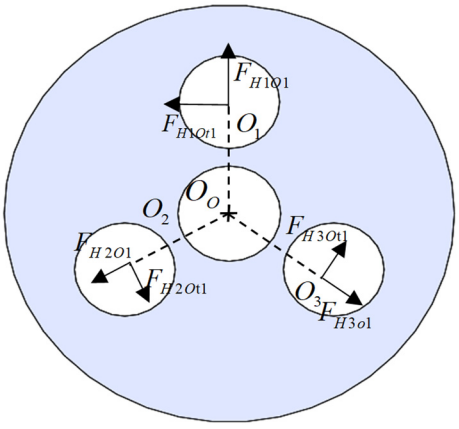

Figure 6. Force analysis of the output disk

(3)Output Plate.The forces exerted by the crankshafts on the output plate carrier are decomposed as follows: F_{Hiot1}, F_{Hiot2},F_{Hiot3} represent the tangential components, while F_{Hio1},F_{Hio2},F_{Hio3} represent the radial components. The output plate remains in equilibrium under the combined action of these crankshaft forces and the external load torque. Therefore, the static equilibrium equations for the output plate are:

$$\sum_{i=1}^{2}\left(F_{Hiot1}+F_{Hiot2}\right)\left(r_s+r_p\right)=T_o \tag{13}$$

From the deformation compatibility conditions, the following can be derived:

$$\begin{cases}\dfrac{F_{1ot1}}{K}=\dfrac{F_{1ot2}}{K}=\dfrac{F_{1ot3}}{K}\\ \dfrac{F_{2ot1}}{K}=\dfrac{F_{2ot2}}{K}=\dfrac{F_{2ot3}}{K}\end{cases} \tag{14}$$

(4) Crankshaft. As shown in Figure 8, each crankshaft is in a state of static equilibrium under the combined action of forces from the planetary gear, the cycloidal gear, and the carrier. Therefore, for the i-th crankshaft, the static equilibrium equations are as follows:

$$\begin{cases}F_{pHit}+\sum_{j=1}^{2}F_{cjHi1}+(F_{oHit1}+F_{oHit2})=0\\ F_{pHi}+\sum_{j=1}^{2}[F_{cjHi2}\cos\beta+F_{cjHi3}\cos(\dfrac{\pi}{2}-\beta)+(F_{oHi1}+F_{oHi1})]=0\end{cases} \tag{15}$$

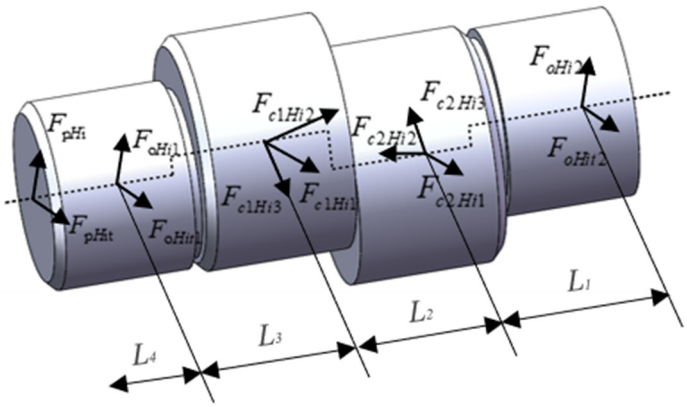

Figure 7. Force analysis of the crankshaft

3. NUMERICAL SIMULATION

3.1. Effect of Errors on Bearing Forces

By combining the equations presented above, the force distribution across each component can be determined.The main structural parameters of the selected RV reducer prototype are listed in Table 1 as follows:

Table 1. Structural Parameters of the RV Reducer

Main Parameters	Unit	Value
Sun Gear Teeth Count: Z_1	——	15
Planetary Gear Teeth Count: Z_2	——	69
Cycloidal Gear Teeth Count: Z_3	——	39
Pin Teeth Count: Z_4	——	40
Eccentricity: l_a	mm	2.2
Module: m	——	1.5

By combining the aforementioned static equilibrium equations and solving them via MATLAB programming for a given counterclockwise rotation angle of the crankshaft, the dynamic variation characteristics of the forces on the key bearings with respect to the crankshaft rotation angle can be obtained for an RV reducer in the presence of errors.By combining the static equilibrium equations and deformation compatibility conditions, numerical simulations were conducted with varying magnitudes of radial and angular errors to determine their influence on the forces acting on each component.

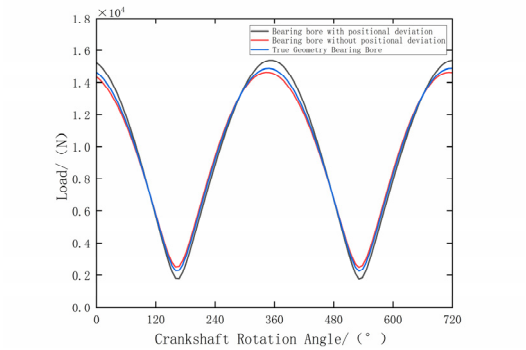

G=0.001mm

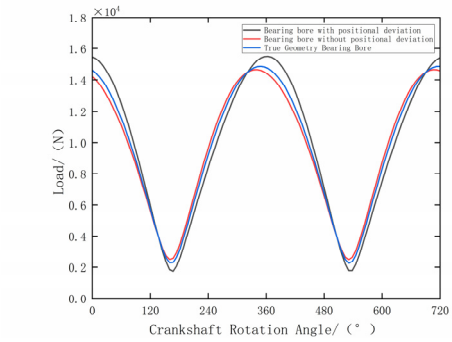

G=0.003mm

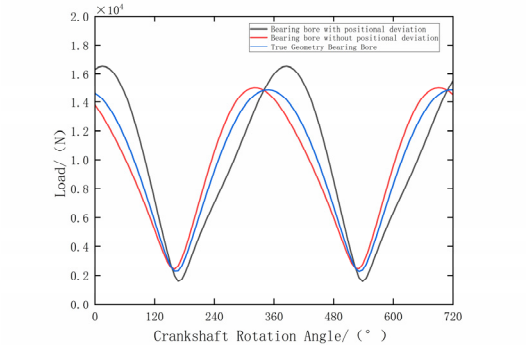

G=0.01mm

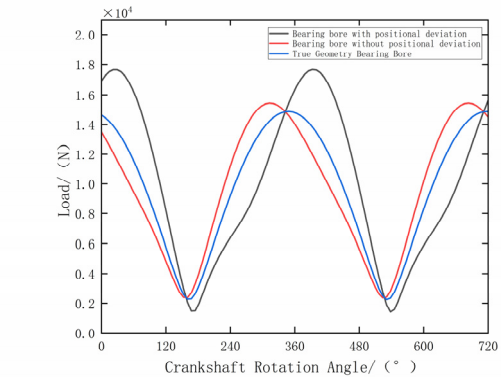

G=0.015mm

Figure 8. Crankpin bearing force with radial error in the bearing bore

Numerical simulations were conducted using different scenarios of radial and angular errors to determine their influence on the forces acting on each component.

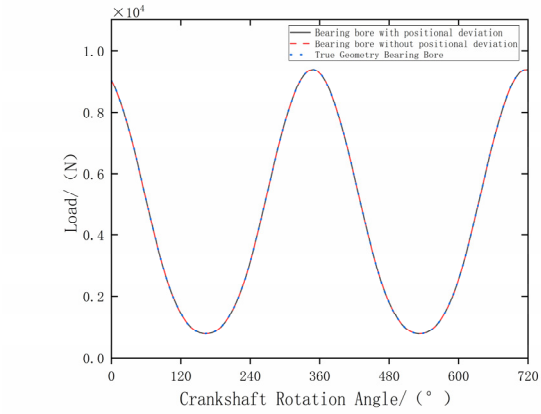

Figure 9. Output bearing force with radial error in the bearing bore

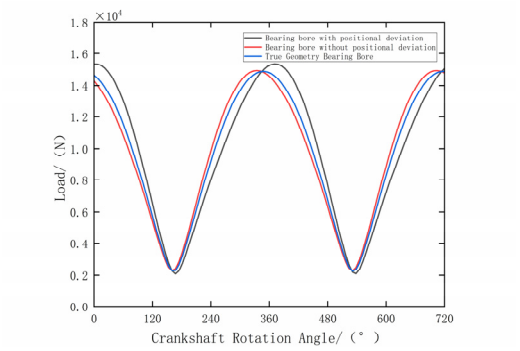

γ=5″

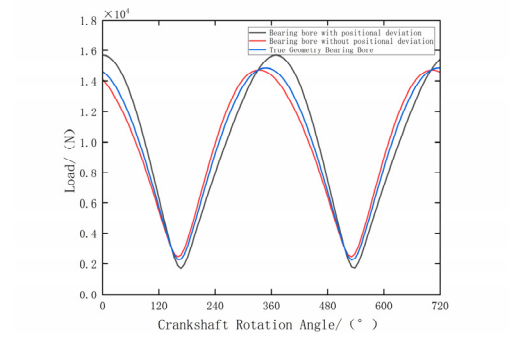

γ=10″

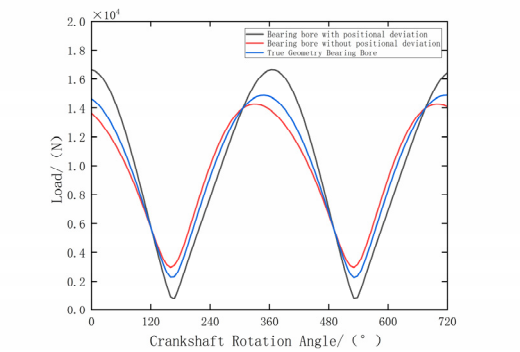

γ=15″

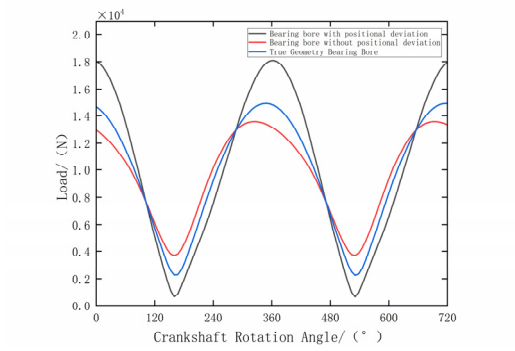

γ=30″

Figure 10. Force on the output bearing with only angular error in the bearing bore

By altering only the magnitude of the radial error while keeping the angular error constant, the effect of radial error on component forces was obtained, as shown in Figure 2-15. The variation in radial error significantly influences the forces on the crankpin bearings. As the radial error increases, the force difference between crankpin bearings with manufacturing errors in the crankshaft bores and the ideal state increases. Their stress amplitude also increases and exceeds that of the ideal condition. In contrast, the force difference between crankpin bearings without manufacturing errors and the ideal state also increases, but their stress amplitude gradually decreases and remains lower than that of the

ideal state. An excessively large radial error may slightly affect the force period. The influence on the output bearing force is minimal and therefore negligible.

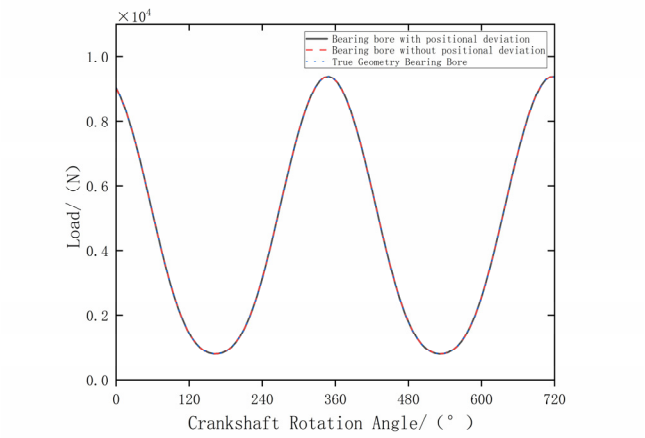

Figure 11. Output bearing force with angular error in the bearing bore

By altering only the magnitude of the angular error while keeping the radial error constant, the effect of angular error on component forces was obtained, as shown in Figure 2-11. The variation in angular error significantly influences the forces on the crankpin bearings. As the angular error increases, the force difference between crankpin bearings with manufacturing errors in the crankshaft bores and the ideal state increases. Their stress amplitude also increases and exceeds that of the ideal condition. In contrast, the force difference between crankpin bearings without manufacturing errors and the ideal state also increases, but their stress amplitude gradually decreases and remains lower than that of the ideal state. The influence on the output bearing force is minimal and therefore negligible.

3.2. Effect of Component Parameters on Forces

Neglecting errors in the reducer, the influence of key component parameters on bearing forces is analyzed.

3.2.1. Effect of Eccentricity on Component Forces

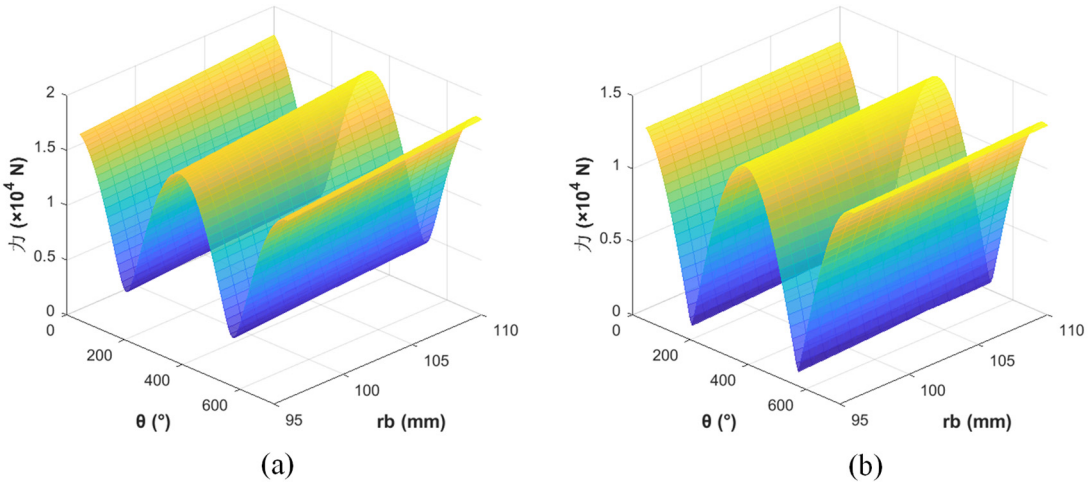

(a)Crankpin bearing force (b)Support bearing force

Figure 12. Effect of Eccentricity

Under the premise of keeping other parameters of the transmission system constant, altering the eccentricity allows for an in-depth investigation into its specific impact on the forces within key components. The analysis results are shown in Figure 3-10. The study found that variations in the eccentricity value do not alter the periodic nature of how the bearing forces change with the crankshaft rotation angle. The maximum force on the crankpin bearings gradually decreases as the eccentricity increases, which is beneficial for reducing the peak load on the bearings. However, the minimum force first decreases and then increases, indicating the existence of an optimal range. Similarly, the maximum force on the support bearings also decreases with increasing eccentricity, while its minimum force initially shows a slight decrease before gradually rising.

3.2.2. Effect of Pin Gear Center Circle Radius on Component Forces

By systematically varying the radius of the pin gear center circle while keeping other structural parameters constant, the influence of this parameter on the bearing forces was analyzed. The specific results are shown in Figure 3-11. The analysis indicates that, similar to the influence of eccentricity, the variation of the short-width coefficient does not alter the periodic pattern of how component forces change with the crankshaft rotation angle. This further confirms that the rotation angle is the fundamental variable determining the force variation pattern. In terms of bearing forces, the crankpin bearings and the support bearings exhibit different response characteristics. As the short-width coefficient changes, both the maximum and minimum forces on the crankpin bearings show a gradually increasing trend. For the output bearings, their maximum and minimum forces also display a gradually increasing trend; however, compared to the crankpin bearings, the rate of increase is relatively slower. Compared to the short-width coefficient, the radius of the pin gear center circle has a relatively smaller influence on the bearing forces.

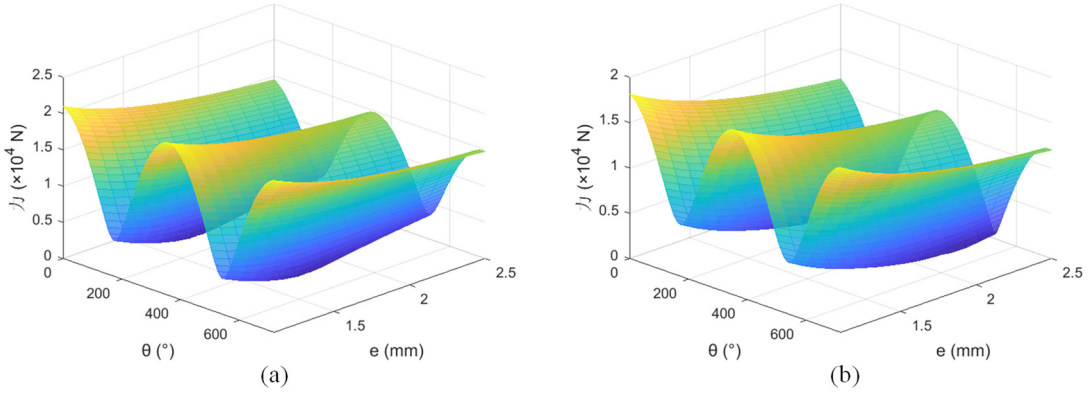

(a)Crankpin bearing force (b)Support bearing force

Figure 13. Effect of the Pin Gear Center Circle Radius

4. SUMMARY

This study establishes a complete static model of the RV reducer, incorporating deformation compatibility and force equilibrium equations, to systematically analyze the force characteristics of its bearing system under the influence of manufacturing errors and key structural parameters. The main conclusions are:

Significant impact of manufacturing errors: Radial and angular errors significantly increase the force amplitude and alter the load distribution on crankpin bearings, while their effect on output bearings is negligible.

Clear influence of structural parameters: Increasing the eccentricity and the pin gear center circle radius can effectively reduce the peak load on the bearings; however, the influence of changes in the pin gear center circle radius on the force trend is weaker compared to that of the eccentricity.

CONFLICTS OF INTEREST

The authors declare that they have no conflict of interest.

REFERENCES

[1] Li Lixing, He Weidong, Wang Xiuqi, Li Chengbo, Wu Ziwei, Fang Rong. Research on High-Precision RV Transmission for Robots[J]. Journal of Dalian Railway Institute, 1999(02): 3-5.

[2] He Weidong, Shan Lijun. Research Status and Prospects of RV Reducers [J]. Journal of Dalian Jiaotong University, 2016, 37(05): 13-18.

[3] He Weidong, Shan Lijun. Research Status and Prospects of RV Reducers [J]. Journal of Dalian Jiaotong University, 2016, 37(05): 13-18.

[4] Wu Suzhen, He Weidong, Zhang Yinghui. Analysis of Force and Contact Characteristics of Crankpin Bearings in RV Transmission Mechanisms [J]. Journal of South China University of Technology (Natural Science Edition), 2020, 48(6): 25-33.

[5] Zheng Yuxin, Xi Ying, Li Mengru, et al. Analysis of Transmission Force Influence in RV Reducers Based on Intimate Value Method [J]. Chinese Journal of Construction Machinery, 2017, 15(02): 153-157+164. DOI: 10. 15999/ j. cnki.311926.2017.02.011.

[6] Cheng Cheng. Structural Analysis of RV Reducers and Research on Bearing Reliability [D]. Jinan: Shandong Jianzhu University, 2020: 10-19.

[7] Xiang Zhaosen, Zheng Peng. Force Analysis of Precision RV Reducers [J]. Internal Combustion Engine & Parts, 2021, (09): 47-49. DOI: 10.19475/j.cnki.issn1674-957x.2021.09.022.